UNIVERSIDAD DISTRITAL
FRANCISCO JOSÉ DE CALDAS

Tecnura

https://revistas.udistrital.edu.co/index.php/Tecnura/issue/view/1201

DOI: https://doi.org/10.14483/22487638.19197

INVESTIGACIÓN

Cooperative strategy to reduce path length in risky environments

Estrategia cooperativa para reducir la longitud de la ruta en entornos riesgosos

José Andrés Chaves Osorio [1], Jimy Alexander Cortés Osorio [2], Edward Andrés González Ríos [3]

Fecha de Recepción: 14 de marzo de 2022 **Fecha de Aceptación**: 12 de diciembre de 2022

Cómo citar: Chaves-Osorio, J.A., Cortés-Osorio, J.A., González-Ríos, E.A. (2023). Cooperative strategy to reduce path length in risky environments. *Tecnura*, **27**(78), 42-72. https://doi.org/10.14483/22487638.19197

Abstract

Objective: Design an artificial intelligence system based on information from the environment that can recommend the shortest path to an individual or vehicle, or robot that moves between two points with the lowest risk of contagion with coronavirus COVID-19.

Methodology: The cooperative strategy for path reduction involves a management and monitoring system and two explorer agents. Explorer agents are equipped with path planning algorithms (GBFS and A*) enhanced with incremental heuristics in order to find two different sets of preliminary paths (the first in direction start-goal and the second in the opposite direction). Subsequently, a management and monitoring system estimates a preliminary shortest path for each path planner then obtains a shortest path by comparing the paths attained with the path planners. This research emerges within the field of distributed intelligence in robotics to determine the benefits of teamwork interactions compared to individual work. In this study, 300 tests that involve the cooperative strategy were executed using ten different environments.

Results: The results of this paper illustrate that in 79% of analyzed situations, definitive shortest estimated paths obtained by cooperative strategy outperformed preliminary paths found individually by path planners. Over 20.5% of tested cases yielded significant path reductions (greater than 100% in relation to the shortest definitive path).

Conclusions: In this work, an artificial intelligence system was designed, whose tests show a good performance. The intelligent system uses Distributed Intelligence implemented in a cooperative team formed by a management and monitoring

[1]PhD in Engineering, Magister in Physical instrumentation, Electrical engineer. Professor in Basic Sciences and Engineering Faculties, Co-Director of research group Robótica Aplicada. Faculty of Basic Sciences, Universidad Tecnológica de Pereira. Pereira, Risaralda, Colombia.
Email: jachaves@ utp.edu.co

[2]PhD in Engineering, electrical engineer. Professor in Physics department, Director of research group Robótica Aplicada. Faculty of Basic Sciences, Universidad Tecnológica de Pereira. Pereira, Risaralda, Colombia.
Email: jacoper@utp.edu.co

[3]Magister in Physical instrumentation, Electronics engineer. Professor in Mechatronic Engineering, researcher in the research group Robótica Aplicada. Faculty of Basic Sciences, Universidad Tecnológica de Pereira. Pereira, Risaralda, Colombia.
Email: edangonzalez@utp.edu.co

system and two explorer agents, who, based on information from the environment, recommend the shortest path to an individual or vehicle or robot who wants to travel between two points located in an environment at risk of contagion with coronavirus COVID-19.
Financing: This work was supported in part by the Universidad Tecnológica de Pereira through Vicerrectoría de Investigaciones Innovación y Extensión, Project name: Sistema de obtención de rutas más seguras bajo situación de pandemia caso covid-19, Project code: 3-20-11, and in part by the Universidad nacional de Colombia.

Keywords: Agent-based modeling, autonomous robots, collaborative work, collision avoidance, cooperative systems, multi-agent systems, navigation, path planning.

RESUMEN

Objetivo: Diseñar un sistema de inteligencia artificial que con base a información del entorno pueda recomendar la ruta más corta a un individuo que quiera desplazarse entre dos puntos con el menor riesgo de contagio con coronavirus COVID-19.
Metodología: La estrategia cooperativa para la reducción de rutas involucra un sistema de administración y monitoreo y dos agentes exploradores. Los agentes exploradores están equipados con algoritmos de planificación de rutas (GBFS y A*) mejorados con heurísticas de tipo incremental a fin de encontrar dos conjuntos diferentes de rutas preliminares (la primera en dirección inicio-meta y la segunda en dirección opuesta). Posteriormente, el sistema de administración y monitoreo estima de forma preliminar el camino más corto para cada planificador de rutas y luego se obtiene el camino más corto comparando los caminos obtenidos con cada uno de los planificadores de rutas. Esta investigación surge dentro del campo de la inteligencia distribuida en robótica para determinar los beneficios de las interacciones del trabajo en equipo frente al trabajo individual. En este estudio se ejecutaron 300 pruebas que involucran la estrategia cooperativa utilizando diez ambientes diferentes.
Resultados: Los resultados de este artículo ilustran que en el 79% de las situaciones analizadas, las rutas estimadas más cortas obtenidas por la estrategia cooperativa fueron aún más cortas que las rutas preliminares encontradas individualmente por los planificadores de rutas. Adicionalmente, en más del 20,5 % de las pruebas realizadas se obtuvieron reducciones de ruta significativas (superiores al 100 % en relación con la ruta más corta).
Conclusiones: En este trabajo se diseñó un sistema de inteligencia artificial, cuyas pruebas muestran un buen desempeño. El sistema inteligente utiliza Inteligencia Distribuida implementada en un equipo cooperativo formado por un sistema de administración y monitoreo y dos agentes exploradores, los cuales, con base a información del entorno, recomiendan el camino más corto a un individuo o vehículo o robot que quiera desplazarse entre dos puntos ubicados en un entorno con riesgo de contagio de coronavirus COVID-19.
Financiamiento: Este trabajo es financiado en parte por la Universidad Tecnológica de Pereira a través del VIIE, Nombre del proyecto: sistema de obtención de rutas más seguras bajo situación de pandemia caso covid-19, Código del proyecto: 3-20-11 y en parte por la Universidad Nacional de Colombia.

Palabras clave: Modelado basado en agentes, robots autónomos, trabajo colaborativo, evasión de colisiones, sistemas cooperativos, sistemas multiagente, navegación, planificación de rutas.

1 INTRODUCTION

Currently, humanity is being subjected to a health emergency of enormous proportions due to the SARS-CoV2 coronavirus pandemic and the associated disease COVID-19 (Islam & Islam, 2020); (Jamshidi *et al.*, 2020). According to the information given by the World Health Organization (WHO), as of 6 March 2022, over 433 million confirmed cases and over 5.9 million deaths had been reported globally. After a couple of years in quarantine and due to significant economic and social needs, there is a glimpse of the possibility that governments allow citizens to leave their homes under specific security protocols. Therefore, it is essential to take advantage of the outbreak places information, as zones with the highest number of infected to evaluate the risk of contagion based on these data. The robotics has been relevance in the context of COVID, as presented by (20) Vargas-Pard et al. (2022), in their work about review of the robotics in the context of COVID healthcare. Their work explores various aspects, such as robotic assistance in patient care, disinfection and cleaning tasks, telemedicine, and remote monitoring. The review highlights the advantages of robotics, including reduced human contact, enhanced efficiency, and improved safety for healthcare workers. The authors conclude that robotics plays a crucial role in mitigating the impact of the pandemic by providing innovative solutions in healthcare delivery.

(Becerra-Mora & Arbulu-Saavedra, 2022) presents an Algorithm for Facility Layout Optimization that is significant in route planning by minimizing distances and flow times in the production chain. Although not explicitly designed for COVID-19, this optimization method holds the potential for managing the pandemic by efficiently organizing resource and equipment distribution in healthcare facilities. The study highlights the importance of researching this topic and the potential contributions various works in route planning can make.

(Martínez-Valencia *et al.*, 2021) presented a methodology for motion planning in autonomous systems with multiple agents; even though it was not aiming to contribute to COVID-19 route planning and mitigation strategies, it could alternatively contribute to covid mitigation in terms of route planning. The proposed methodology parameterized the physical behavior of autonomous navigation systems and implements a control policies algorithm. The methodology proposed in their paper showcases its effectiveness in motion planning for autonomous systems with multiple agents. This

methodology can enhance the efficiency and effectiveness of COVID-19 route planning and mitigation efforts by providing optimal solutions and mitigating challenges associated with multiple agent systems.

This work presents a process to obtain the shortest path between two points and thus minimizes the time and the distance of exposure of people or vehicles traveling through different risky scenarios. The recommended path can be provided to users through vehicle navigation systems, a smartwatch, or a smartphone.

Distributed intelligence in autonomous exploration robots: One of the challenges of autonomous exploration robots is to displace safely from the starting point to the arrival point in the shortest possible path (Amanatiadis *et al.,* 2013); (Chonnaparamutt & Birk, 2006); (Liu *et al.,* 2013); (5) Murphy, 2004; (11)Ponticelli Lima, 2010; (12) RamaKrishna, Sowmya Bala, S. N. Chakravarthy, Bhanu Prakash Sarma, & Sai Alla, 2012; (21) Vilela, Liu, & Nejat, 2013). Safety requirements imply the completion of tasks avoiding collisions, falling into holes, and mine detonations, among other risks. With this goal in mind, researchers have provided robots with specialized hardware and software. The evolution of software has been significant in that it has allowed the implementation of artificial intelligence (AI) (Kuhnt *et al.,* 2016). AI algorithms afford robots a certain level of decision-making capabilities, e.g., path planning algorithms (Estlin *et al.,* 2001); (3)Mac, Copot, Tran, & De Keyser, 2016). However, AI implementation demands the use of high processing and memory resources. Additional hardware requirements increase manufacturing costs of exploration robots. Said investment might be lost during dangerous tasks such as rescuing people in collapsed structures. Distributed intelligence (DI) has emerged as a less expensive option; for instance, the division of the main task into subtasks can be tackled by specific members of a team. The concept of capacity distribution not only helps in cost reduction, but also leads to better results in comparison to tasks performed by an individual. DI systems performance relies on the type of interactions of the individuals: collective, collaborative, coordinative or cooperative (9)(Parker, 2008). In the next section, some of this concepts are described that are relevant for the implementation of the techniques presented in this paper.

Directed graph: A graph (G) is composed of a set of elements called cross points (C), and a set of relationships called arcs (A). Formally, graphs can be represented as an ordered pair of sets (1)

$$G(C, A) \tag{1}$$

For practical purposes, $C_1, C_2, C_3, \ldots, C_n$, are defined as elements of C, as shown in (2).

$$C = \{C_1, C_2, C_3, \ \ldots, \ C_n\} \tag{2}$$

On the other hand, an arc can be considered as a set of three elements (C_i, C_j, l_{ij}), which establishes a relationship between the crossing points C_i and C_j, a sense of the relationship between the points $(C_i \rightarrow C_j)$, and a value or associated length (L_{i-j}). The graphic form of an arc is illustrated in Figure 1 (Guichard, n.d.); (J.s & M.R., 1996); (6) Murray-Lasso, 2003).



Fig. 1. Representation of an arc in a graph, adapted to introduce the notation used in this study.

Source: *Authors*

Simple directed graphs are highly recommended to represent path maps, which in turn favor the solution proposed herein and its implementation at the software level. Figure 2 shows a simple directed graph with four nodes $(C_1, C_2, C_3$ and $C_4)$, and three edges $(L_{1-2}, L_{2-3}, L_{3-4})$.

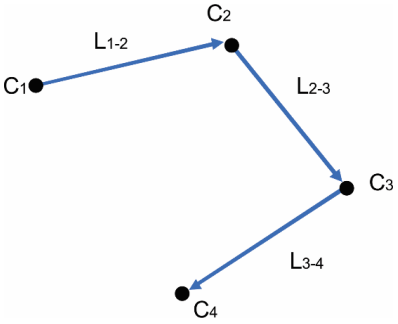


Fig. 2. Simple directed graph with four nodes (C_1, C_2, C_3, C_4) and three edges $(L_{1-2}, L_{2-3}, L_{3-4})$, adapted to explain the proposal in this study.

Source: *Authors*

Path planning: Path planning is a relevant topic in autonomous mobile robot research (Cho & Cho, 2014); (Espitia Cuchango & Sofrony Esmeral, 2012); (García *et al.*, 2007); (Latombe, 2012); (López García, 2011); (8) Ospina, Garzán, & Baldomiro, 2011). As the robots must perform tasks in the best conditions, some of the principal requirements for the path planners are (Bruce & Veloso, 2003); (Garrido *et al.*, 2007a); (Garrido *et al.*, 2007b); (Laumond *et al.*, 1994); (LaValle, 1998); (1)López, Gómez-Bravo, Cuesta, & Ollero, 2006; (19)Vargas, 2007): 1. Displacement from the starting to the arrival

point, 2. Safety displacement and 3. Obtaining the least-costly path. In this study, two explorer agents equipped with A* and GBFS (Greedy Best First Search Algorithm) path planners determine the path without collisions thanks to offset programming and sensors that detect obstacles. Later, the Shortest Estimated Path (SEP) will be obtained by a Monitoring and Management System (MMS), which will be introduced in Section II. The A* path planner was used because of its widespread use in Robotics literature (Fortune & Wilfong, 1991) ; (Koenig & Likhachev, 2002); (Koenig *et al.*, 2004a); (Kumar Das *et al.*, 2011); (2) Lozano-Pérez & Wesley, 1979; (7)Murray & Sastry, 1993; (15)Spangelo & Egeland, 1994; (16) Stentz, 1995) and, additionally, researchers have reported the following strengths: low consumption of processing resources, easy implementation, and simple programming changes (Duchon *et al.*, 2014); (Fernández, 2005); (Goyal & Nagla, 2014); (Koenig *et al.*, 2004a); (Konakalla, 2014); (4)Muntean, 2016; (13)Russell & Norvig, 2016; (14)Singh, Sharma, Sutton, Hatton, & Khan, 2018; (17)Sundfeld, Razzolini, Teodoro, Boukerche, & de Melo, 2018)The GBFS path planner was used due to a common base of construction with A* algorithm, which facilitates comparisons between them (Heusner *et al.*, 2018).

Gbfs algorithm (greedy best first search algorithm): The heuristic function of the GBFS Algorithm given by the equation (3).

$$f\left(n\right) = h\left(n\right) \tag{3}$$

Takes into account the following parameters:

n, nodes of the space to explore.

h(n), estimate of the distance from the current position of the explorer agent to the desired position. This estimate is obtained from concepts such as Euclidean or Manhattan distances, depending on the specific application. In this study Euclidean distances are used.

A* algorithm (a star algorithm): The heuristic function of algorithm A* takes into account the same parameters considered in the GBFS and includes a new one, *g(n)*. The typical heuristic function for A* is shown in equation (4).

$$f\left(n\right) = h\left(n\right) + g(n) \tag{4}$$

The *g(n)* function estimates the cost of moving from the initial node to any other node (10)(Patel's, s/f). Finally, *f(n)* let's find the path with the lowest cost. Considering the aforementioned information, we present a cooperative strategy for the estimation of the shortest path from a starting point

to an arrival point by a team of autonomous robots. Slight differences among exploration agents are due to respective algorithms and settings of initial operating conditions. The results obtained herein present the shortest paths by cooperative strategy in comparison to those by each robot working individually (18)(Sunehag et al., 2018). The rest of this paper is structured as follows: The methods section presents a proposal of new variants of the GBFS and A* used in a Cooperative Strategy for Path Length Decrease (CSPLD), and their validation procedure. The results and discussion section describes a detailed analysis of one simulated environment and the measurement of the cooperative strategy contribution to obtain the SEP in 100 tests in ten different simulated environments. Finally, conclusions and future works sections are presented.

2 METHODOLOGY

Proposal of new variants of gbfs and a*: In order to prevent returns to an already visited node and to guarantee simple directed graphs, the authors added a new element *p(n)* to heuristic functions of the GBFS and A* algorithms. This is done by increasing the total cost function *f(n)* by adding a cost function *p(n)* to each node already visited (the chosen value of *p(n)* is 1). Equations (5) and (6) represent the enhanced heuristic functions for the GBFS and A*, respectively are.

$$f\left(n\right) = h\left(n\right) + p(n) \tag{5}$$

$$f\left(n\right) = h\left(n\right) + g\left(n\right) + p(n) \tag{6}$$

The heuristic functions are applied to each of the eight successor positions around the current position, but only the one containing the smallest value of *f(n)* will be chosen as the next best position. Algorithm 1 and algorithm 2, shows the pseudocodes for new path planners IH-GBFS and IH-A*, respectively.

Pseudocode for algorithm IH-GBFS.

textbfInivar()⇒ Initialize

1: $E = MXN$
2: $Vroute = [\,]$
3: $n = n_s \in E$

C()⇒ Cost function

4: $h(n', n_g) = d_E(n', n_g)$
5: $C(n, n') = f(n, n') = h(n) + p(n)$

Planif()⇒ Search process

6: $n' = Succ(n)$
7: $Vroute = C(n, n')\ \forall n' \in E$
8: $Bp_i = min(Vopen) \in E$
9: $n = n'_i \mid n_i \exists\ Bp_i \in E$
10: $return(n)$

Main()⇒ Main process

11: $Inivar()$
12: **for(1)**
13: $Planif()$
14: **if(n==ng)**
15: End of the search
16: **End if**
17: Update vertex
18: **End for**

Algorithm 1. Pseudocode for algorithm IH-GBFS.

Pseudocode for algorithm IH-A*.

Inivar()⇒ Initialize

1: $E = MXN$
2: $Nopen = [\,]$
3: $Nclose = 0$
4: $Vopen = [\,]$
5: $n = n_s \in E$

AddNopen()⇒ Update open nodes

6: $Nopen = [Nopen, n \in E]$

AddNclose()⇒ Update close nodes

7: $Nopen.r(n)$
8: $NClose = [Nclose, n]$

C()⇒ Cost function

9: $h(n', n_g) = d_E(n', n_g)$
10: $g(n, n') = d_E(n, n') + g^*(n, n')$
11: $C(n, n') = f(n, n') = h(n) + g(n) + p(n)$

Planif()⇒ Search process

12: $n' = Succ(n) \in Nopen$
13: $Vopen = C(n, n')\ \forall n' \in E$
14: $Bp_i = min(Vopen) \in E$
15: AddNclose(n)
16: $n = n'_i \mid n_i \exists\ Bp_i \in E$
17: $return(n)$

Main()⇒ Main process

18: $Inivar()$
19: **for(1)**
20: $AddNopen$
21: $Planif()$
22: **if(n==ng)**
23: End of the search
24: **End if**
25: Update vertex
26: **End for**

Algorithm 2. Pseudocode for algorithm IH-A*.

A characteristic of the algorithms created by the authors is the retrieval of past events for each exploration agent, thus upgrading to incremental heuristic algorithms (IH-GBFS and IH-A*) (Koenig *et al.*, 2004b).

Cooperative strategy for path length decrease: Initially, in this section, two concepts will be defined: strategy and the cooperative process. Then, the Cooperative Strategy for Path Length Decrease (CSPLD) will be explained. A strategy is considered a detailed method or plan, chosen to achieve a goal or to solve a problem under conditions of uncertainty. A strategy describes how the goal will be achieved, whether its attainment depends exclusively on a fixed plan or the systems it is able to adapt to in its environment, according to the emergence of a particular pattern of activity. Since available resources are usually limited, the strategy resorts to the planning and organization of resources for an efficient and effective implementation. A strategy generally involves setting goals, determining actions to achieve those goals, and mobilizing resources to execute the actions (Freedman, 2015). A cooperative process is a type of DI, in which a team of agents works in unison to plan, solve problems, and learn (Hussein, 2018); (9)Parker, 2008). In this team, every member is aware of the other team members. The individual actions of each member of the cooperative team support the attainment of the main goal (Aljehani & Inoue, 2019); (Kim *et al.*, 2015). A team of two exploration agents and an MMS carries out the CSPLD, whose scheme is illustrated in Figure 3.

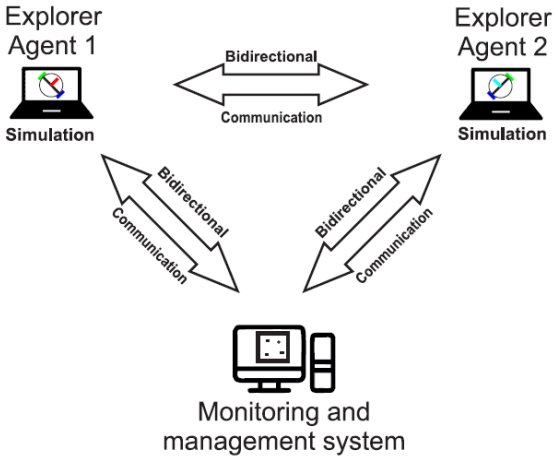


Fig. 3. Communication framework among two agents and the MMS applying the CSPLD to obtain the SEP.

Source: *Authors*

Each exploration agent uses its own path planner to create a path between start and goal points (Alje-

hani & Inoue, 2019). After the path planning process, each agent knows the position of its teammate. In order to obtain the SEP from data provided by the agents, the MMS computes, compares and combines paths of each agent (if possible) following the rules in Table 1.

Table 1. CSPLD cases and actions to determine SEP.

Source: *Authors*

No.	CASES	SEP ACTIONS
1	The two paths obtained are exactly the same.	**a. SEP selection:** The first path is chosen as the final path and designated as the SEP. Alternatively, the second path could be chosen based on different decision criteria such as fewer nodes, less control effort, or lower energy consumption during traversal.
2	The two paths obtained are different from each other, with equal traveled distances and no intersections.	
3	The two paths obtained are different from each other, with different traveled distances and no intersections.	**a. SEP selection:** The path with the shortest traveled distance is chosen as the SEP.
4	The two paths obtained are different from each other, with equal traveled distances and crossings in some sections.	**a. Crossing points location:** Crossing points are identified as (C1, C2, ..., Ci, Cj, ..., Cn). **b. Section definition:** A section is defined as the portion of paths between crossing points Ci and Cj.
5	The two paths obtained are different from each other, with different traveled distances and intersections in some sections.	**c. Comparison of paths:** The traveled distances of agents are compared in each section, and the shortest one is selected. **d. Combination of paths:** The concatenation of previously selected paths with the shortest distances results in the definitive path called SEP.

As seen in Table 1, each case matches a corresponding action, aiming to obtain the SEP. From the five

situations compared, only cases 4 and 5 imply path combinations; and only the fifth obtains a different SEP from previous paths found by exploration agents. Figure 4 corresponds to a representative environment of the fifth case. The dark and thick margin represents the offset associated with the border of the environment.

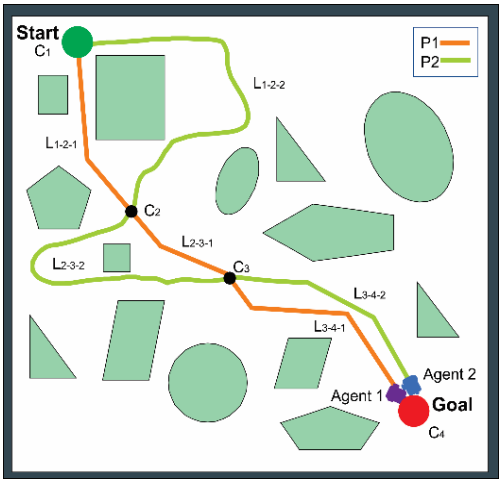


Fig. 4. Two agents and their paths (obtained with their respective path planners) are shown in a representative situation of the fifth case. This situation is used to explain the combination of paths in this study.

Source: *Authors*

For display effects to find the SEP, the following notation is defined (see Figure 4.):

$P1$: Orange path generated by agent 1.

$P2$: Green path generated by agent 2.

i: First sub index indicating the crossing point that precedes a path section, i=1to n-1.

j: Second sub index indicating the crossing point at the end of a path section, $j = 2$ to n.

k: Third sub index identifies agents, a path belongs to $k = 1$ or $k = 2$ (Agent 1 or 2 respectively).

C_i: Crossing point, from lowest (1) to highest (n), along the paths of agents $1, 2$.

L_{i-j-k}: Arc length traveled by agent k between crossing points C_i and C_j forming a path section.

S: Start point (C_1).

G: Goal point (C_4).

According to the previous notation in Figure 4, equation (7) and equation (8) are obtained.

$$P1 = L_{1-2-1} + L_{2-3-1} + L_{3-4-1} \tag{7}$$

$$P2 = L_{1-2-2} + L_{2-3-2} + L_{3-4-2} \tag{8}$$

Table 2 compares the sections of paths P1 and P2 between common crossing points of Figure. 4.

Table 2. Comparisons between the common sections of path P1 and path P2.

Source: *Authors*

Cross points	Section of P1	Comparison	Section of P2
$C_1 - C_2$	L_{1-2-1}	$<$	L_{1-2-2}
$C_2 - C_3$	L_{2-3-1}	$<$	L_{2-3-2}
$C_3 - C_4$	L_{3-4-1}	$>$	L_{3-4-2}

Equation (9) shows the result of the addition of the shortest path sections reported in Table 2. Moreover, Figure. 5 shows the SEP obtained by the CSPLD.

$$SEP = L_{1-2-1} + L_{2-3-1} + L_{3-4-2} \tag{9}$$

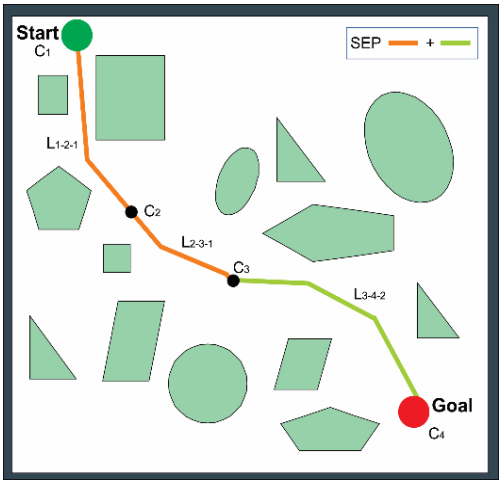


Fig. 5. Graphic example of the SEP obtained by the CSPLD implementation.

Source: *Authors*

Although Table 2 shows a particular solution (see Figure 4 and Figure 5) to find the SEP between P1 and P2, it is possible to generalize the same SEP procedure equation (9) for paths that have n crossing points in common (including the start and goal). In order to achieve such a generalization, j needs to be redefined in terms of i as shown in equation (10).

$$j = i + 1 \tag{10}$$

Finally, using the equation (10), the generalization of equation (9) is given by equation (11).

$$SEP = \sum_{i=0}^{n-2} min(l_{i-(i+1)-1}, l_{i-(i+1)-2}) \tag{11}$$

The generalization in equation (11) implies, at the software level, that all the cases previously described in Table 1 can be subject to the complete procedure of the SEP actions programmed for the fifth case in Table 1.

Validation procedure: This section validates the CSPLD effectiveness at the software level, whose mathematical formulation is given by equation (11). First, for the tests, IH-GBFS, IH-A* and MMS algorithms were coded in Matlab R2016a, running in Windows 10 on a Dell T7600 computer with an Intel Xeon processor of 2.40 GHz and installed RAM of 16 GB. Ten different environments with ten different positions of both start-to-goal points, were tested, resulting in 100 simulations of the cooperative strategy. Each test environment consists of a grid of 100 x 100 cells (as seen in Figure 6). Black cells represent obstacles, white cells correspond to empty spaces, and blue cells indicate the programmed offset to avoid collisions with the border of the obstacles (14). Green and red squares represent specific positioning of start and goal points respectively.

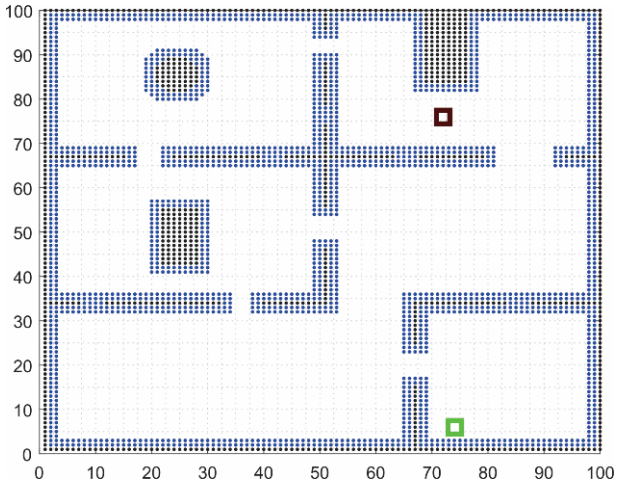


Fig. 6. Example of environment setting for the CSPLD simulations. In this study, the environment is labeled with the number 10, and is described as a two-dimensional square box of 100 cells per 100 cells, which has walls, free spaces, and three objects (one circle and two rectangles). This environment represents a house that has five rooms without doors. In two rooms, there is a rectangular object. In one room, there is a circular object.

Source: *Authors*

The implementation entails additional commutation of start and goal points, which leads to 200 partial SEP's before obtaining the definitive 100 SEP's. The results presented in the following subsection are summarized in tables with the subsequent nomenclature:

P1A: Distance from start to goal with path planner IH-A* (in cell units).

P1B: Distance from goal to start with path planner IH-A* (in cell units).

P2A: Distance from start to goal with path planner IH-GBFS (in cell units).

P2B: Distance from goal to start with path planner IH-GBFS (in cell units).

Data gathered from the 10 environments were subject to a four-table comparative analysis, whose most relevant estimations are as follows:

SEP P1: Distance of the partial SEP after applying cooperative strategy to P1A and P1B (in cell units).

SEP P2: Distance of the partial SEP after applying cooperative strategy to P2A and P2B (in cell units).

SEP: Distance of the definitive SEP after applying cooperative strategy to SEP P1 and SEP P2 (in cell units).

Finally, a percentage of the decreased length of original paths (P1A and P2A) in relation to the definitive SEP is obtained.

3 RESULTS AND DISCUSSION

Detailed analysis of one selected environment: Since the cooperative strategy and the type of collected data were the same for the ten tested environments, only detailed information corresponding to environment 10 will be presented for the sake of illustration (see Figure 6). This environment seeks to resemble a house that has five no-door rooms, in which three of them have a regular-sized object.

1. Data associated to the SEP P1 are found in Table 3. The first column in Table 3, identifies 10 different positions of start and goal points. Additionally, Table 3 illustrates percentages of the decreased path length given by equation (12) and equation (13), respectively. Figure 7 is an example (corresponding to test 5) comparing a partial SEP P1 with original P1A and P1B.

Table 3. The SEP P1 by cooperative strategy for environment 10.

Source: *Authors*

Test	Path length (cells)			% Decrease of path length	
	P1A	P1B	SEP P1	%P1A-SEP P1	%P1B-SEP P1
1	109.31	343.56	106.38	2.75	222.94
2	112.14	105.90	105.90	5.89	0.00
3	97.74	305.32	97.74	0.00	212.38
4	116.38	107.66	107.66	8.11	0.00
5	150.38	100.97	95.70	57.14	5.51
6	116.23	134.23	116.23	0.00	15.49
7	108.80	108.80	101.77	6.91	6.91
8	117.38	348.88	117.38	0.00	197.21
9	522.49	116.14	116.14	349.87	0.00
10	98.77	99.94	87.05	13.46	14.80

Where:

$$\%P1A - SEP\ P1 = \left| \frac{SEP\ P1 - P1A}{SEP\ P1} \right| * 100\% \tag{12}$$

$$\%P1B - SEP\ P1 = \left| \frac{SEP\ P1 - P1B}{SEP\ P1} \right| * 100\% \tag{13}$$

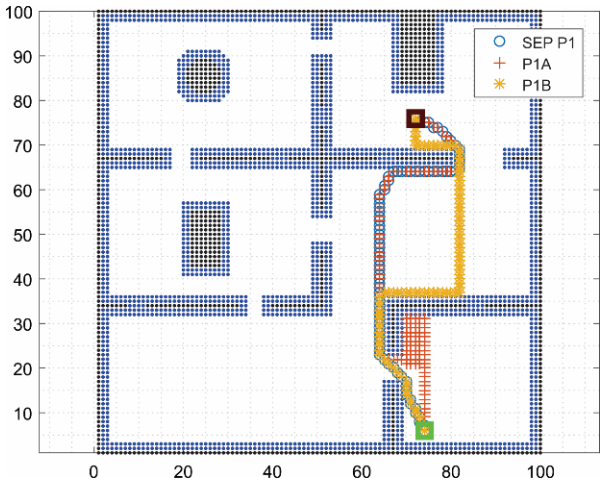


Fig. 7. The SEP P1 obtained by the CSPLD from P1A and P1B for environment 10, test 5

Source: *Authors*

2. Data associated with the SEP P2 are found in Table 4. The first column identifies 10 different positions of start and goal points. Additionally, Table 4 illustrates percentages of the decreased path length given by equation (14) and equation (15), respectively. Figure. 8 is an example (corresponding to test 5) comparing the partial SEP P2 with the original P2A and P2B.

Table 4. The SEP P2 by cooperative strategy for environment 10.

Source: *Authors*

Test	Path length			% Decrease of path length	
	P2A	P2B	SEP P2	%P2A-SEP P2	%P2B-SEP P2
1	219.84	353.98	112.08	96.14	215.82
2	114.87	114.87	106.08	8.28	8.28
3	97.74	435.83	97.74	0.00	345.91
4	123.36	151.60	109.40	12.76	38.58
5	764.12	651.76	97.18	686.27	570.65
6	132.61	164.51	132.61	0.00	24.06
7	108.80	108.80	101.77	6.91	6.91
8	479.62	379.68	379.68	26.32	0.00
9	345.18	106.18	100.33	244.06	5.84
10	138.67	171.74	87.05	59.29	97.28

Where:

$$\%P2A - SEP\ P2 = \left| \frac{SEP\ P2 - P2A}{SEP\ P2} \right| * 100\% \tag{14}$$

$$\%P2B - SEP\ P2 = \left| \frac{SEP\ P2 - P2B}{SEP\ P2} \right| * 100\% \tag{15}$$

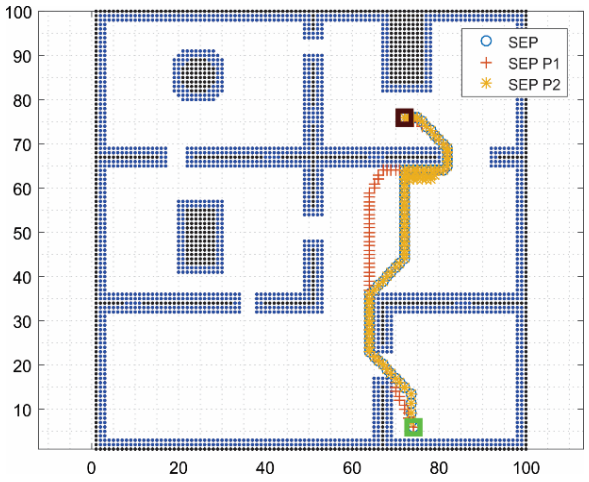


Fig. 8. The SEP P2 obtained by the CSPLD from P2A and P2B for environment 10, test 5.

Source: *Authors*

3. Data associated with the definitive SEP are found in Table 5. The first column identifies 10 different start and goal positioning points. Additionally, the table reports percentages of the decreased path length given by equation (16) and equation (17) respectively. Figure 9 is an example (corresponding to test 5) comparing the definitive SEP against the SEP P1 and the SEP P2.

Table 5. The definitive SEP by cooperative strategy for environment 10.

Source: *Authors*

Test	Path length			% Decrease of path length	
	SEP P1	SEP P2	SEP	%SEP P1-SEP	%SEP P2-SEP
1	106.38	112.08	106.38	0.00	5.36
2	105.90	106.08	102.77	3.05	3.22
3	97.74	97.74	97.74	0.00	0.00
4	107.66	109.40	104.14	3.37	5.05
5	95.70	97.18	80.11	19.45	21.31
6	116.23	132.61	116.23	0.00	14.10
7	101.77	101.77	101.77	0.00	0.00
8	117.38	379.68	105.08	11.71	261.31
9	116.14	100.33	100.33	15.76	0.00
10	87.05	87.05	87.05	0.00	0.00

Where:

$$\%SEP1 - SEP = \left| \frac{SEP - SEP\ P1}{SEP} \right| * 100\% \tag{16}$$

$$\%SEP2 - SEP = \left| \frac{SEP - SEP\ P2}{SEP} \right| * 100\% \tag{17}$$

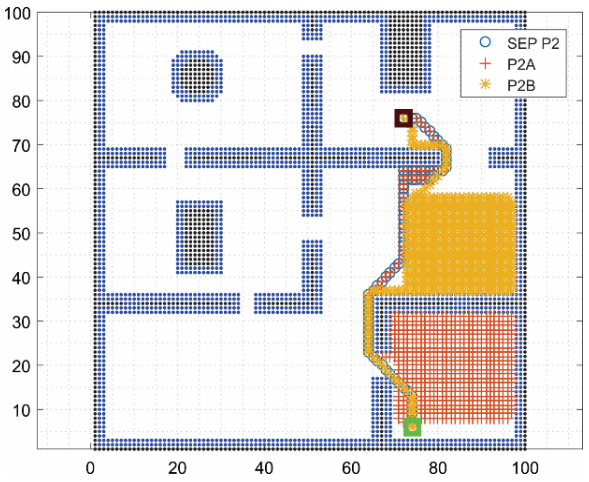


Fig. 9. The SEP obtained by the CSPLD from SEP P1 and SEP P2 for environment 10, test 5.

Source: *Authors*

4. The last two columns of Table 6 illustrate the percentage of the decreased length of original paths (P1A and P2A) with the definitive SEP obtained by equation (18) and equation (19), respectively.

Table 6. Comparison of the P1A and P2A paths vs the SEP using a cooperative strategy in environment 10.

Source: *Authors*

Test	Path length			% Decrease of path length	
	P1A	P2A	SEP	%P1-SEP	%P2-SEP
1	109.31	219.84	106.38	2.75	106.65
2	112.14	114.87	102.77	9.12	11.77
3	97.74	97.74	97.74	0.00	0.00
4	116.38	123.36	104.14	11.76	18.45
5	150.38	764.12	80.11	87.72	853.81
6	116.23	132.61	116.23	0.00	14.10
7	108.80	108.80	101.77	6.91	6.91
8	117.38	479.62	105.08	11.71	356.42
9	522.49	345.18	100.33	420.80	244.06
10	98.77	138.67	87.05	13.46	59.29

Where:

$$\%P1A - SEP = \left| \frac{SEP - P1A}{SEP} \right| * 100\% \tag{18}$$

$$\%P2A - SEP = \left| \frac{SEP - P2A}{SEP} \right| * 100\% \tag{19}$$

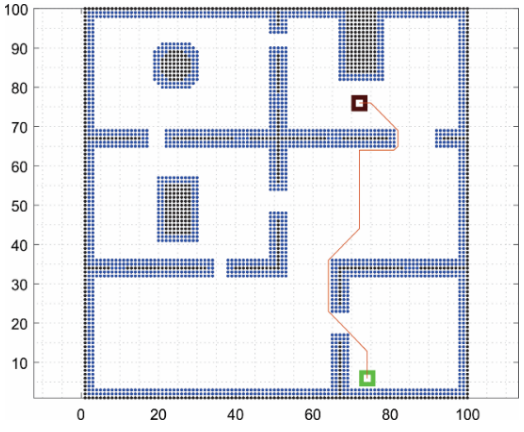


Fig. 10. The definitive SEP obtained in environment 10, test 5

Source: *Authors*

For the authors, cases with percentages greater than 0.00 are labeled as “successful”, i.e., the CSPLD was capable of obtaining shorter paths in comparison to the ones initially given by path planners.

Figure 10 illustrates the definitive SEP for environment 10, test 5. As a last note, zeros reported in tables should not be regarded as results of implementation of the cooperative strategy without the MMS involvement. Indeed, null reductions of paths are only revealed after the MMS processing of information is provided by explorer agents.

Measurement of cooperative strategy contribution: Since the last decrease percentages (Table 6) are relevant to measure the contribution of this methodology, the tables of this section compile this indicator for the ten tested environments and their corresponding tests (100 tests for each of the two path planners). Said compilation will be presented from two different perspectives. The first compilation criterion selected is success "S", i.e., the number of tests in which the CSPLD achieved a decrease in the path length with respect to the original individual path planning (decrease percentages greater than 0.00). The second criterion to measure the contribution is called "%PKA-SEP", defined by the authors as the percentage of path decrease given by an agent K, between start and goal points in relation to the definitive SEP. Tables 7, 8 and 9 detail necessary information to assess the cooperative strategy according to the "success" criterion. Tables associated with this evaluation use the following nomenclature:

%S/IH-A*: Percentage of the CSPLD success with respect to the individual work of the IH-A* path planner.

Table 7. Percentages of CSPLD success with respect to the individual work of the path planners.

Source: *Authors*

Environment	**Tests**	**S**	
		%S/IH-A*	**%S/IH-GBFS**
1	1-10	90	80
2	11-20	90	90
3	21-30	90	70
4	31-40	90	80
5	41-50	90	100
6	51-60	50	40
7	61-70	80	70
8	71-80	80	70
9	81-90	80	70
10	91-100	80	90

After comparing information provided by Table 7, the CSPLD achieved a path reduction in most environments (at least in 70% of tests). However, tests on environment 6 diverged from this high rate of success, with a less successful reduction rate of 50 % of S/IH-A* and 40 % of S/IH-GBFS. The divergent results in environment 6 were due to some unchallenging positioning of start and goal points for this particular environment (depicted in Figure 11), proof of which is that this same environment presented three PA1–SEP percentages above 500% (see Figure 12).

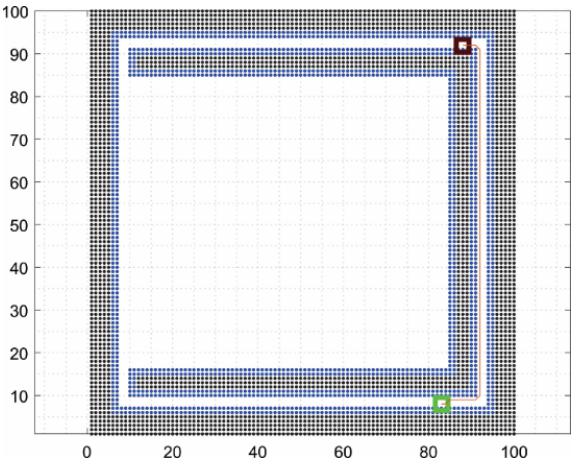


Fig. 11. Unchallenging positioning of start and goal points in setting of environment 6.

Source: *Author*

By averaging percentages of Table 7, the overall success of the whole experiment is given in Tables 8 and 9. The new tables have the following nomenclature:

%S/Path planner: Percentage of the total CSPLD success with respect to the individual work of each path planner.

%S: Percentage of the total CSPLD success in the experiment.

Table 8. Percentage of the total CSPLD success about the individual work of each path planner IH-GBFS and IH-A*.

Source: *Authors*

	Tests	**%S/Path planner**	
		IH-A*	**IH-GBFS**
Total 10 environments	100	82	76

Table 9. . Percentage of the CSPLD performance in relation to the individual work of the path planners IH-GBFS and IH-A*.

Source: *Authors*

	Tests	**%S**
Total	200	79

The CSPLD assessment based on the %PKA-SEP criterion requires the proportion of each de-

crease in percentage of the original path obtained by agent K in comparison to its corresponding definitive SEP. For such a purpose, Figure 12 illustrates reduction peaks, and zones of null reduction for all the ten tested environments and their respective ten tests (100 tests in total shown in the horizontal axis of Figure12). In Figure 12, the blue dotted line identifies reductions of the CSPLD in relation to IH-A*. The red line corresponds to reductions of the CSPLD in relation to IH-GBFS. Figure 12 illustrates a clear disparity between the most challenging least challenging environments for both planners (considering the particular start and goal positioning points). On tests 28 to 53, four significant peaks converge above 400% of the %PKA-SEP; conversely, in tests 55 to 60 and 67 to 70 two dips are noticed, in which the %PKA-SEP is zero or has a very low percentage of path decrease. With the purpose of giving the reader an idea of the general impact of the CSPLD, 20.5% of the performed tests obtained a SEP with reductions over 100% of the %PKA-SEP. Therefore, a definitive SEP by the CSPLD can be significantly shorter than the original path planned by IH-A* and IH-GBFS.

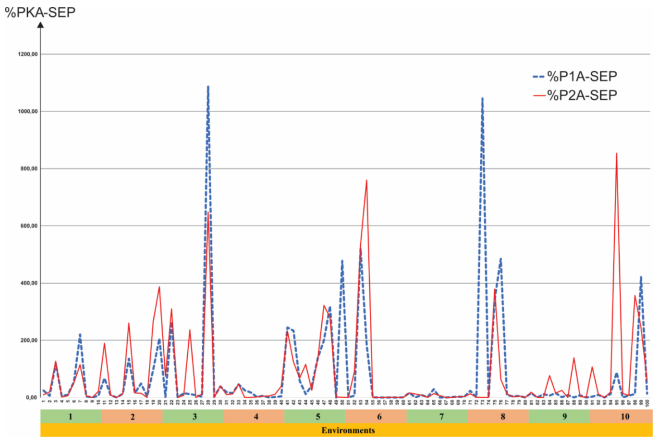


Fig. 12. CSPLD assessment based on %PKA-SEP.

Source: *Authors*

Even though it has not been tested in real environments, this research presents a promising strategy that holds potential for effectively safeguarding populations. While further validation in real-world scenarios is needed, the developed artificial intelligence system, with its distributed intelligence approach and utilization of heatmap and contour lines, shows promise in mitigating risks in COVID-19-prone environments. Its successful performance in simulations indicates the viability of employing this strategy for protecting populations from potential contagion threats.

Using the positions of hidden marks found in Figure 13(a) and using Equation 20 (considering $u = 1$);

are created simulations of R in Matlab; as seen in Figure 13 (b), and Figure 13 (c). Figure 13 (b) shows a top view of the Risk potential in a hot diagram (see colour scale) and Figure 13 (c) shows the Risk potential field, because of hidden marks found in Figure 13 (a).

$$R = \sum_{i=1}^{m} \frac{u}{d_j}; 0 < R < \infty \tag{20}$$

Where:

j: subscript describing the number of the mark found between a group from 1 to m

m: Total number of "hidden marks found"

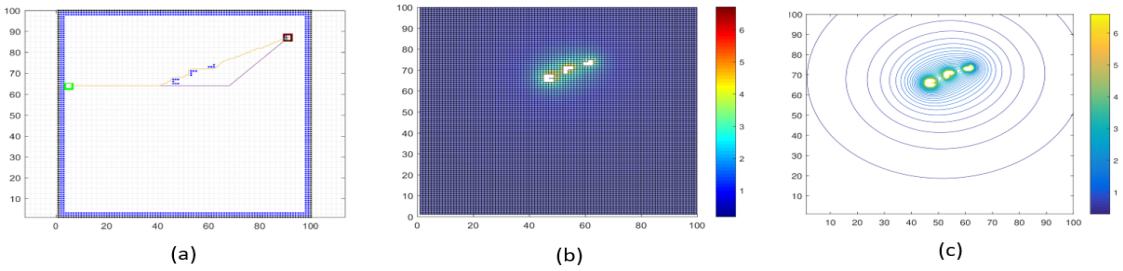


Fig. 13. (a) The initial point is colored green, and the target point is black. Additionally, three Covid-19 risk points are colored blue. (b) The heatmap in this figure illustrates the proximity risk around each point. (c) Lastly, the figure presents contour lines indicating areas with the same level of risk.

Source: *Authors*

4 Conclusions

In the analyzed environments, the CSPLD exhibited a significant rate of success overall, since it yielded path reductions for 79% of the 200 cases analyzed. The only environment diverging from this behavior demonstrates a "moderate" rate of success (45%) with a more challenging positioning of start and goal points. As far as path planners are concerned, the CSPLD achieved higher rates of success for IH-A* cases (82%) in comparison to those of IH-GBSF (76%). The overall rate of success in terms of path planners was 79%. Regarding the % PKA-SEP, it is evident that 14% of performed tests obtained a SEP with reductions of over 200%. Therefore, the definitive SEPs by the CSPLD can be significantly shorter than the original paths, planned by IH-A* and IH-GBFS. The aforementioned convergences of peaks point to the most challenging cases for both planners. The two algorithms

were quite inefficient in relation to the CSPLD. In these cases, the CSPLD delivered severe corrections to their original paths. In other words, the greatest contributions of the methodology were achieved in these cases. The dips defined above represent the least challenging specific cases for both planners. In these cases, the CSPLD offered slight corrections (under 10% of the %PKA-SEP). In other words, the less significant contributions of the methodology were demonstrated in these cases. Since the highest values of the %PKA-SEP were achieved in environments that challenged the algorithms individually, in these environments the potential of the CSPLD is revealed.

5 FUTURE WORKS

As a continuation of this study, explorer agents could work with different algorithms (e.g., Bug, D* or DFS) or, perhaps, modifications, such as interactions among path planners. Likewise, a collaborative interaction of the DI system can be selected, in which an agent could warn others about obstacles.

6 FUNDING

This work is funded in part by the Universidad Tecnológica de Pereira through the VIIE, Project Name: "Sistema de obtención de rutas más seguras bajo situación de pandemia caso covid-19," Project Code: 3-20-11, and in part by the Universidad Nacional de Colombia.

REFERENCES

Aljehani, M., & Inoue, M. (2019). Performance evaluation of multi-UAV system in post-disaster application: Validated by HITL simulator. *IEEE Access*, *7*. https://doi.org/10.1109/ACCESS.2019.2917070

Amanatiadis, A. A., Chatzichristofis, S. A., Charalampous, K., Doitsidis, L., Kosmatopoulos, E. B., Tsalides, P., ... Roumeliotis, S. I. (2013). A multi-objective exploration strategy for mobile robots under operational constraints. *IEEE Access*, *1*. https://doi.org/10.1109/ACCESS.2013.2283031

Becerra-Mora., Y.A. y Arbulu-Saavedra, M.R. (2022). Uso de robótica en una emergencia sanitaria. *Tecnura*, *26 núm 73*, 130-141. https://doi.org/10.14483/22487638.17320

Bruce, J., & Veloso, M. M. (2003). Real-time randomized path planning for robot navigation. En *Lecture Notes in Artificial Intelligence (Subseries of Lecture Notes in Computer Science)* (Vol. 2752). https://doi.org/10.1007/978-3-540-45135-8_23

Cho, K. B., & Cho, S. Y. (2014). The concept of collision-free motion planning using a dynamic collision map. *International Journal of Advanced Robotic Systems*, *11*. https://doi.org/10.5772/58707

Chonnaparamutt, W., & Birk, A. (2006). Using rescue robots to increase construction site safety. En *2006 Proceedings of the 23rd International Symposium on Robotics and Automation in Construction, ISARC 2006*. https://doi.org/10.22260/isarc2006/0047

Duchon, F., Babinec, A., Kajan, M., Beno, P., Florek, M., Fico, T., & Jurišica, L. (2014). Path planning with modified A star algorithm for a mobile robot. En *Procedia Engineering* (Vol. 96). https://doi.org/10.1016/j.proeng.2014.12.098

Espitia Cuchango, H. E., & Sofrony Esmeral, J. I. (2012). Algoritmo para planear trayectorias de robots móviles, empleando campos potenciales y enjambres de partículas activas brownianas. *Ciencia e Ingeniería Neogranadina*, *22*(2). https://doi.org/10.18359/rcin.242

Estlin, T., Volpe, R., Issa, N., Mutz, D., Fisher, F., Engelhardt, B., & Chien, S. (2001). Decision-Making in a Robotic Architecture for Autonomy. International Conference on Intelligence Analysis. https://ai.jpl.nasa.gov/public/papers/isairas01-estlin.pdf

Fernández, M. (2005). Algoritmos de búsqueda heurística en tiempo real. Aplicación a la navegación en los juegos de video.EST. https://users.exa.unicen.edu.ar/catedras/aydalgo2/docs/TFca06aCompleto.pdf

Fortune, S., & Wilfong, G. (1991). Planning constrained motion. *Annals of Mathematics and Artificial Intelligence*, *3*(1). https://doi.org/10.1007/BF01530887

Freedman, L. (2015). *Strategy: A history*. Oxford University Press.

García, D. A. L., Bravo, F. G., & del Toro Peral, M. (2007). Comparativa entre planificadores de trayectorias para su uso combinado en la generación de maniobras. https://rabida.uhu.es/dspace/bitstream/handle/10272/5501/Nuevas_aportaciones_en_algoritmos_de_planificacion.pdf?sequence=2

Garrido, S., Moreno, L., Blanco, D., & Munoz, M. L. (2007). Sensor-based global planning for mobile robot navigation. En Robotica (Vol. 25). https://doi.org/10.1017/S0263574707003384

Garrido, Santiago, Moreno, L., Blanco, D., & Martin, F. (2007). Exploratory navigation based on voronoi transform and fast marching. En *2007 IEEE International Symposium on Intelligent Signal Processing, WISP*. https://doi.org/10.1109/WISP.2007.4447541

Goyal, J. K., & Nagla, K. S. (2014). A new approach of path planning for mobile robots. En *Proceedings of the 2014 International Conference on Advances in Computing, Communications and Informatics, ICACCI 2014*. https://doi.org/10.1109/ICACCI.2014.6968200

Guichard, D. (s/f). Combinatorics and Graph Theory. Department of Mathematics Whitman College. https://www.whitman.edu/mathematics/cgt_online/book/

Heusner, M., Keller, T., & Helmert, M. (2018). Search progress and potentially expanded states in greedy best-first search. En *IJCAI International Joint Conference on Artificial Intelligence* (Vol. 2018-July). https://doi.org/10.24963/ijcai.2018/735

Hussein, A. A. M. (2018). Control and communication systems for automated vehicles cooperation and coordination. http://hdl.handle.net/10016/27674

Islam, M. N., & Islam, A. K. M. N. (2020). A Systematic Review of the Digital Interventions for Fighting COVID-19: The Bangladesh Perspective. *IEEE Access*, *8*, 114078–114087. https://doi.org/10.1109/ACCESS.2020.3002445

J.s, & M.R. (1996). *Diseño y manejo de estructuras de datos en C*. Mc Graw-Hill Interamericana.

Jamshidi, M., Lalbakhsh, A., Talla, J., Peroutka, Z., Hadjilooei, F., Lalbakhsh, P., … Mohyuddin, W. (2020). Artificial Intelligence and COVID-19: Deep Learning Approaches for Diagnosis and Treatment. *IEEE Access*, *8*. https://doi.org/10.1109/ACCESS.2020.3001973

Kim, C., Yang, H., Kang, D., & Lee, D. (2015). 2-D cooperative localization with omni-directional mobile robots. En *2015 12th International Conference on Ubiquitous Robots and Ambient Intelligence, URAI 2015*. https://doi.org/10.1109/URAI.2015.7358894

Koenig, S., & Likhachev, M. (2002). D* lite. *AAAI/IAAI*, *15*, 476–483.

Koenig, S., Likhachev, M., & Furcy, D. (2004). Lifelong Planning A*. *Artificial Intelligence*, *155*(1–2). https://doi.org/10.1016/j.artint.2003.12.001

Koenig, S., Likhachev, M., Liu, Y., & Furcy, D. (2004). Incremental heuristic search in AI. *AI Magazine*, *25*(2). https://ddn.aaai.org/AAAI/2002/AAAI02-072.pdf

Konakalla, S. V. (2014). A Star Algorithm. unpublished. http://cs.indstate.edu/~skonakalla/paper.pdf

Kuhnt, F., Pfeiffer, M., Zimmer, P., Zimmerer, D., Gomer, J. M., Kaiser, V., … Zöllner, J. M. (2016). Robust environment perception for the audi autonomous driving cup. En *IEEE Conference on Intelligent Transportation Systems, Proceedings, ITSC*. https://doi.org/10.1109/ITSC.2016.7795744

Kumar Das, P., Patro, S. N., Panda, C. N., & Balabantaray, B. (2011). D* lite algorithm based path planning of mobile robot in static Environment. *Int. J. Comput. Commun. Technol.(IJCCT)*, *2*, 32–36. http://dx.doi.org/10.47893/IJCCT.2012.1158

Latombe, J.-C. (2012). *Robot motion planning* (Vol. 124). Springer Science \& Business Media.

Laumond, J. P., Jacobs, P. E., Taïx, M., & Murray, R. M. (1994). A Motion Planner for Nonholonomic Mobile Robots. *IEEE Transactions on Robotics and Automation*, *10*(5). https://doi.org/10.1109/70.326564

LaValle, S. M. (1998). Rapidly-Exploring Random Trees: A New Tool for Path Planning. *In*, *129*. https://msl.cs.illinois.edu/~lavalle/papers/Lav98c.pdf

Liu, Y., Nejat, G., & Vilela, J. (2013). Learning to cooperate together: A semi-autonomous control architecture for multi-robot teams in urban search and rescue. En *2013 IEEE International Symposium on Safety, Security, and Rescue Robotics, SSRR 2013*. https://doi.org/10.1109/SSRR.2013.6719367

López, D., Gómez-Bravo, F., Cuesta, F., & Ollero, A. (2006). Planificación de trayectorias con el algoritmo RRT. Aplicación a robots no holónomos. *Revista Iberoamericana de Automática e Informática Industrial*, *3*(3), 56–67. https://www.polipapers.upv.es/index.php/RIAI/article/view/8144

López García, D. A. (2011). *Nuevas aportaciones en algoritmos de planificación para la ejecución de maniobras en robots autónomos no holónomos*. http://hdl.handle.net/10272/5501

Lozano-Pérez, T., & Wesley, M. A. (1979). An Algorithm for Planning Collision-Free Paths Among Polyhedral Obstacles. *Communications of the ACM*, *22*(10). https://doi.org/10.1145/359156.359164

Mac, T. T., Copot, C., Tran, D. T., & De Keyser, R. (2016). Heuristic approaches in robot path planning: A survey. *Robotics and Autonomous Systems*, *86*. https://doi.org/10.1016/j.robot.2016.08.001

Martínez-Valencia., J.L. Holguín-Londoño., M. y Ramírez-Vanegas., C.A. (2021). Methodology for the Synthesis of Automata in the Planning of Movements for Autonomous Systems with Multiple Agents. *Tecnura*, 25(70), 46-70. https://doi.org/10.14483/22487638.17131

Muntean, P. (2016). Mobile robot navigation on partially known maps using a fast a star algorithm version. *arXiv preprint arXiv:1604.08708*. https://doi.org/10.48550/arXiv.1604.08708

Murphy, R. R. (2004). Trial by fire [rescue robots]. *IEEE Robotics & Automation Magazine*, *11*(3). https://doi.org/10.1109/MRA.2004.1337826

Murray-Lasso, M. A. (2003). Math puzzles, powerful ideas, algorithms and computers in teaching problem-solving. *Journal of Applied Research and Technology*, *1*(03). https://doi.org/10.22201/icat.16656423.2003.1.03.606

Murray, R. M., & Sastry, S. S. (1993). Nonholonomic motion planning. Steering using sinusoids. *IEEE Transactions on Automatic Control*, *38*(5). https://doi.org/10.1109/9.277235

Ospina, A. G., Garzán, C., & Baldomiro, H. (2011). Diseño, implementación y aplicación de una estrategia de búsqueda preferente por amplitud, para uso multidireccional sobre sistemas distribui-

dos o de procesamiento en paralelo, usando un simulador de escenarios, construido para el trazado de rutas en robots. https://hdl.handle.net/11059/2609

Parker, L. E. (2008). Distributed Intelligence: Overview of the Field and its Application in Multi-Robot Systems. *Journal of Physical Agents*, *2*(1). https://doi.org/10.14198/JoPha.2008.2.1.02

Patel's, A. (s/f). Stanford, California, USA. Recuperado el 3 de agosto de 2019, de https://www.redblobgames.com/pathfinding/a-star/introduction.html

Ponticelli Lima, R. C. (2010). Sistema de exploración de terrenos con robots móviles: aplicación en tareas de detección y localización de minas antipersonas.

RamaKrishna, A., Sowmya Bala, G., S. N. Chakravarthy, A., Bhanu Prakash Sarma, B., & Sai Alla, G. (2012). Design of a Rescue Robot Assist at Fire Disaster. *International Journal of Computer Applications*, *47*(10). https://doi.org/10.5120/7225-0056

Russell, S. J., & Norvig, P. (2016). Artificial intelligence: a modern approach. Malaysia. Pearson Education Limited London, UK.

Singh, Y., Sharma, S., Sutton, R., Hatton, D., & Khan, A. (2018). A constrained A* approach towards optimal path planning for an unmanned surface vehicle in a maritime environment containing dynamic obstacles and ocean currents. *Ocean Engineering*, *169*, 187–201. https://doi.org/10.1016/j.oceaneng.2018.09.016

Spangelo, I., & Egeland, O. (1994). Trajectory Planning and Collision Avoidance for Underwater Vehicles Using Optimal Control. *IEEE Journal of Oceanic Engineering*, *19*(4). https://doi.org/10.1109/48.338386

Stentz, A. (1995). Optimal and efficient path planning for unknown and dynamic environments. *International Journal of Robotics and Automation*, *10*(3). https://doi.org/10.1007/978-1-4615-6325-9_11

Sundfeld, D., Razzolini, C., Teodoro, G., Boukerche, A., & de Melo, A. C. M. A. (2018). PA-Star: A disk-assisted parallel A-Star strategy with locality-sensitive hash for multiple sequence alignment.

Journal of Parallel and Distributed Computing, *112*. https://doi.org/10.1016/j.jpdc.2017.04.014

Sunehag, P., Lever, G., Gruslys, A., Czarnecki, W. M., Zambaldi, V., Jaderberg, M., et al. (2018). Value-decomposition networks for cooperative multi-agent learning based on team reward. En *Proceedings of the International Joint Conference on Autonomous Agents and Multiagent Systems, AAMAS* (Vol. 3). https://doi.org/10.48550/arXiv.1706.05296

Vargas, H. C. (2007). Generación de trayectorias para un robot móvil Khepera II usando técnicas de aprendizaje automático. https://www.repositoriodigital.ipn.mx/bitstream/123456789/5703/1/Tesis12175.pdf

Vargas-Pardo, L.F. y Giraldo-Ramos, F.N. (2022). Firefly Algorithm for Facility Layout Optimization. *Tecnura*, 26(74), 35-48. https://doi.org/10.14483/22487638.17731

Vilela, J., Liu, Y., & Nejat, G. (2013). Semi-autonomous exploration with robot teams in urban search and rescue. En *2013 IEEE International Symposium on Safety, Security, and Rescue Robotics, (SSRR 2013)*. https://doi.org/10.1109/SSRR.2013.6719366